

Robust Uncertainty Bounds in Reproducing Kernel Hilbert Spaces: A Convex Optimization Approach

Paul Scharnhorst*, Emilio T. Maddalena*, Yuning Jiang*, Colin N. Jones

Automatic Control Laboratory, École Polytechnique Fédérale de Lausanne,
Route Cantonale, 1015 Lausanne, Switzerland

{paul.scharnhorst,emilio.maddalena,yuning.jiang,colin.jones}@epfl.ch

Abstract

Let a labeled dataset be given with scattered samples and consider the hypothesis of the ground-truth belonging to the reproducing kernel Hilbert space (RKHS) of a known positive-definite kernel. It is known that out-of-sample bounds can be established at unseen input locations, thus limiting the risk associated with learning this function. We show how computing tight, finite-sample uncertainty bounds amounts to solving parametric quadratically constrained linear programs. In our setting, the outputs are assumed to be contaminated by bounded measurement noise that can otherwise originate from any compactly supported distribution. No independence assumptions are made on the available data. Numerical experiments are presented to compare the present results with other closed-form alternatives.

Keywords: Uncertainty bounds, reproducing kernel Hilbert space, robust guarantees.

1 Introduction

We consider the problem of quantifying the uncertainty associated with point-evaluations of an unknown ground-truth map given a dataset of observations and assumptions on its nature. The analysis differs from widespread concentration bounds found in the machine learning literature as no assumptions are made on the statistical independence of samples. This agnosticism is central when dealing with systems that incorporate memory such as physical plants that evolve in a dynamical and hence strongly correlated fashion—see [Schölkopf, 2019] for a thorough discussion on situations where the typical i.i.d. premise is inadequate. In exchange, we pose conditions on the ground-truth, requiring it to belong to a specific class of functions [Cucker and Zhou, 2007], and allow for observations to be scattered, not necessarily being drawn from any specific distribution. This is rather customary in the established field of approximation theory [Schaback, 1995, Wendland, 2004, Iske, 2018]. See also [Belkin, 2018] for a recent perspective on the advantages offered by approximation-type bounds.

The setting in this paper is that of kernel learning, which is among the most prominent modern frameworks for both classification and regression. These non-parametric techniques are usually more data-efficient than deep network architectures, and recently intriguing connections between these two methodologies were established [Mei et al., 2019, Domingos, 2020, De Matthews et al., 2018]. Kernels can be regarded as similarity measures between examples in a certain feature space [Schölkopf et al., 2002]. This space is known as the reproducing kernel Hilbert space (RKHS), and is usually an infinite-dimensional linear space of functions. Moreover, it is well known that the RKHS associated with certain kernel classes is dense in the space of continuous functions on compact domains [Micchelli et al., 2006]. By requiring the latent ground-truth

* The first two authors contributed equally. * Corresponding author: Yuning Jiang.

to be a member of the RKHS associated with a known kernel, straightforward error-bounds can be established for models that interpolate noise-free data-points (see for instance [Schaback and Wendland, 2006]). Recently, these out-of-sample guarantees were extended to regularized smoothing models in the presence of bounded measurement noise [Maddalena et al., 2020b]. Nevertheless, the task of *exactly* quantifying the associated uncertainty in the latter scenario remained open, as well as understanding how much conservativeness is introduced when centering the bounds around pre-specified models.

Contributions: Herein we investigate the uncertainty quantification problem in RKHSs and with datasets corrupted by measurement noise. The sources of uncertainty are both epistemic and aleatoric [O'Hagan, 2004] as respectively explained next. The first stems from the ground-truth being an unknown fixed member of our function class, and from which we derive information indirectly through its samples. Secondly, the additive bounded measurement noise, which could originate from any probability measure, or even be a constant, fixed bias. In contrast with the study in [Maddalena et al., 2020b], we carry out an *algorithmic independent* analysis that is not centered around any specific model; this is done by computing the highest and lowest possible point-evaluations that are consistent with our knowledge. Our main result is to show how this infinite-dimensional problem can be translated into a finite convex quadratically constrained linear program (QCLP) without any conservatism, which is accomplished through a representer theorem. Next, properties of this procedure are derived and connections with the closed-form sub-optimal bounds as well as classical noise-free bounds are established. Finally, efficient solution methods are proposed through the dual optimization problem, which trade-off computational time and precision. Numerical experiments are reported to illustrate their use, as well as the influence of the input distribution on the final results.

Relevance for automatic control: The use of the so-called data-driven techniques to refine models, improve performance on-line, or approximate controllers is becoming evermore present in the field of automatic control [Chakrabarty et al., 2016, Rosolia and Borrelli, 2017, Umlauft and Hirche, 2019]. In the particular case of kernel surrogate models, a considerable body of rigorous literature exists for linear dynamics [Chen et al., 2014, Pillonetto et al., 2014, Pin et al., 2015, Fujimoto et al., 2018], linear parameter-varying dynamics [Rizvi et al., 2018, Laurain et al., 2020], Hammerstein and Wiener cascaded systems [Risuleo et al., 2017, Risuleo et al., 2019], mainly adopting a time-domain perspective of the identification problem. When operational constraints are present, one has to pair these tools with appropriate uncertainty quantification techniques to not make unsafe decisions. Examples include system simulation with guaranteed accuracy [Lauricella and Fagiano, 2020] and controller tuning algorithms that avoid unreliable parameters [Berkenkamp et al., 2016, Lederer et al., 2020]. By establishing our optimal, non-asymptotic uncertainty bounds, our work aims at bridging non-parametric kernel learning and robust analysis and control. Practical applications of the results include predictive control schemes that explicitly incorporate non-parametric uncertainties [Manzano et al., 2020, Maddalena et al., 2020a], and the certification of machine learning-based algorithms [Knuth et al., 2021, Wabersich et al., 2021], but in a deterministic fashion. More generally, the tools provided in this paper could also be employed in robust data-driven optimization [Bertsimas and Koduri, 2021]. Our motivation is similar in essence to the ones found in non-linear set membership and interval analysis works [Raissi et al., 2004, Karimshoushtari and Novara, 2020], but our study is focused on kernel machines and their associated spaces.

Notation: \mathbb{N} denotes the set of natural numbers and \mathbb{R}^d is the d -dimensional Euclidean space. Let S_1 and S_2 be subspaces of S , then $S_1 \oplus S_2 = S$ indicates their vector direct sum, i.e., $\forall s \in S, \exists! s_1 \in S_1, \exists! s_2 \in S_2 : s = s_1 + s_2$. We denote by K_{XX} the matrix of kernel evaluations at X , i.e., the matrix containing $k(x_i, x_j)$ at its i -th row and j -th column, $x_i, x_j \in X$. Let a query point x be specified, then K_{Xx} represents the column vector-valued function $x \mapsto [k(x, x_1) \dots k(x, x_d)]^\top \in \mathbb{R}^d$, whereas K_{xX} denotes its transpose. For a matrix A we denote its nullspace by $N(A)$.

2 Preliminary: Kernels and their native spaces

We start by briefly reviewing the formalism of kernel learning, and define the main elements that will be later used in our analysis. The reader is referred to [Schaback and Wendland, 2006, Manton et al., 2015] for further details on topic.

A kernel $k : \Omega \times \Omega \rightarrow \mathbb{R}$ is any symmetric, real-valued function defined on a non-empty input set Ω . k is said to be positive-definite if the weighted sum $\sum_{i=1}^n \sum_{j=1}^n \alpha_i \alpha_j k(x_i, x_j)$ is strictly positive $\forall n \in \mathbb{N}, \forall \alpha_1, \dots, \alpha_n \in \mathbb{R} \setminus \{0\}, \forall x_1, \dots, x_n \in \Omega$. An example of a commonly used continuous kernel that enjoys this property is the squared-exponential, also known as the radial basis function (RBF) kernel. Associated with each k , there is a unique Hilbert space of maps \mathcal{H} that is referred to as the reproducing kernel Hilbert space (RKHS) or native space of k . For compact domains Ω , [Micchelli et al., 2006] presents families of kernels whose \mathcal{H} are dense in the space of continuous functions, which can be interpreted as a measure of richness of such a space. Let $\mathbb{R}^\Omega = \{f : \Omega \rightarrow \mathbb{R}\}$ and $L_x : \mathbb{R}^\Omega \rightarrow \mathbb{R}$ be the map $L_x : f \mapsto f(x)$, also known as the evaluation functional for a given $x \in \Omega$. Formally, a RKHS is simply a Hilbert space $\mathcal{H} \subset \mathbb{R}^\Omega$ for which the L_x maps are continuous $\forall x \in \Omega$. It turns out that partially-evaluated kernels $k(x, \cdot)$ belong to $\mathcal{H}, \forall x \in \Omega$ and define evaluation functionals through $\langle f, k(x, \cdot) \rangle_{\mathcal{H}} = f(x), \forall f \in \mathcal{H}, \forall x \in \Omega$. The latter is known as the reproducing property. From a constructive viewpoint, \mathcal{H} is given as the closure (w.r.t. the topology induced by the inner-product) of span $(\{k(x, \cdot), x \in \Omega\})$, encompassing thus weighted sums of partial kernels and limit points of sequences as well. It can be shown that this construction results in proper functions and not in equivalence classes of them.

Let $f \in \mathcal{H}$ with finite expansion $f = \sum_{i=1}^{n_f} \alpha_i k(x_i, \cdot)$, $\alpha_i \in \mathbb{R}, x_i \in \Omega$, for all i . Its induced norm $\|f\|_{\mathcal{H}}$ is then given by

$$\|f\|_{\mathcal{H}}^2 = \left\langle \sum_{i=1}^{n_f} \alpha_i k(x_i, \cdot), \sum_{i=1}^{n_f} \alpha_i k(x_i, \cdot) \right\rangle_{\mathcal{H}} = \sum_{i=1}^{n_f} \sum_{j=1}^{n_f} \alpha_i \alpha_j k(x_i, x_j) = \alpha^\top K_{XX} \alpha \quad (1)$$

due to the reproducing property, with α being the vector of scalar weights. If a member $f \in \mathcal{H}$ is the limit of a sequence $f = \sum_{i=1}^{\infty} \alpha_i k(x_i, \cdot)$, then its norm is $\|f\|_{\mathcal{H}}^2 = \lim_{n \rightarrow \infty} \sum_{i=1}^n \sum_{j=1}^n \alpha_i \alpha_j k(x_i, x_j)$. As a last introductory step, we consider a finite subset $X \subset \Omega$ and define the power function $P_X : \Omega \rightarrow \mathbb{R}_{\geq 0}$ as

$$P_X(x) = \sqrt{k(x, x) - K_{XX} K_{XX}^{-1} K_{XX}} \quad (2)$$

whenever clear from the context, the reference to X will be omitted. $P_X(x)$ can be interpreted as a form of statistical covariance, and evaluates to zero $\forall x \in X$.

3 Optimal bounds in RKHSs

Herein we consider a positive-definite kernel $k : \Omega \times \Omega \rightarrow \mathbb{R}$ along with its corresponding RKHS set $\mathcal{H} \subset \mathbb{R}^\Omega$. Our input space is taken to be a compact subset of the Euclidean space $\Omega \subset \mathbb{R}^n$. A dataset $\{(x_i, y_i)\}_{i=1}^d$ is given to us, being composed of inputs $x_i \in \Omega$ and outputs $y_i \in \mathbb{R}^{n_i}, y_i = [y_{i,1} \ \dots \ y_{i,n_i}]^\top$ that contain n_i scalar samples collected at the same input location x_i . The dataset carries information about an underlying ground-truth map $f^* \in \mathcal{H}$ according to

$$y_{i,j} = f^*(x_i) + \delta_{i,j} \quad (3)$$

where $\delta_{i,j}$ represents an additive measurement noise that is assumed to be uniformly bounded by a known scalar quantity $|\delta_{i,j}| \leq \bar{\delta}, \forall i, j$. Furthermore, for notational convenience, we define the quantities $X := \{x_1, \dots, x_d\}$ and $y := [y_1^\top \ \dots \ y_d^\top]^\top$, which represent respectively the collection of inputs and the available outputs.

The aim is to quantify the uncertainty associated with the latent function f^* , confining its point-evaluations $L_x(f^*) = f^*(x)$ in the output space \mathbb{R} . We note that, from the reproducing property and the Cauchy–Schwarz inequality, one can readily establish

$$|f(x)| = |\langle f, k(x, \cdot) \rangle_{\mathcal{H}}| \leq \|f\|_{\mathcal{H}} \|k(x, \cdot)\|_{\mathcal{H}} = \|f\|_{\mathcal{H}} \sqrt{k(x, x)} < \infty \quad (4)$$

$\forall f \in \mathcal{H}$, including the ground-truth. If the kernel k is translation-invariant (also referred to as stationary), $k(x, x)$ is constant $\forall x \in \Omega$ and (4) constitutes a uniform trivial bound for the unknown function. A reason for this inequality to be rather loose is that it does not incorporate any information provided by the dataset or by the measurement bound $\bar{\delta}$, which we exploit next.

Assumption 1. *An estimate $\Gamma \geq \|f^*\|_{\mathcal{H}}$ for the ground-truth norm is known.*

Remark 1. (On the necessity of Γ): Data alone are not sufficient to compute *any* out-of-sample bounds when considering functions $f \in \mathcal{H}$, regardless of the number of samples $d < \infty$ that one has. Given any tentative bound ϵ at $x \notin X$, there exists $f_\rho \in \mathcal{H}$ consistent with the dataset that will violate the bound, that is, $f_\rho(x) > \epsilon + \rho$, for any pre-specified violation level $\rho > 0$. This is simply due to the existence of maps that can interpolate any finite set of samples. Restricting the search to the Γ -ball in \mathcal{H} limits the flexibility of the considered functions, thus allowing for guarantees to be established. An analogous argument can be made in the space of Lipschitz functions [Milanese and Novara, 2004]. If no bound is posed on the Lipschitz constant of the ground-truth, assuming Lipschitz continuity *per se* becomes vacuous. RKHS norms can be estimated from below directly based on data as illustrated in Appendix A.

Consider the following infinite-dimensional variational problem $\mathbb{P}0$, with the query point $x \in \Omega$ as a parameter

$$F(x) = \sup_{f \in \mathcal{H}} \{f(x) : \|f\|_{\mathcal{H}} \leq \Gamma, \|f_X - y\|_{\infty} \leq \bar{\delta}\} \quad (5)$$

where $f_X := \Lambda [f(x_1) \ \dots \ f(x_d)]^\top$ is the vector of evaluations at the input locations, which are repeated whenever multiple outputs are available at a given input. This is accomplished through Λ as defined in Appendix B. We highlight that the supremum is guaranteed to exist thanks to (4). Given a query location x , $\mathbb{P}0$ yields the tightest upper bound for $f(x)$ over all members $f \in \mathcal{H}$ of our hypothesis space that are consistent with our dataset, as well as our knowledge on the ground-truth complexity $\|f\|_{\mathcal{H}} \leq \Gamma$. Note how linking the function evaluations f_X and the outputs y plays a role analogous to conditioning stochastic processes on past observations in statistical frameworks.

Consider now the convex parametric quadratically-constrained linear program $\mathbb{P}1$

$$\begin{aligned} C(x) &= \max_{c \in \mathbb{R}^d, c_x \in \mathbb{R}} c_x \\ \text{subj. to} \quad & \begin{bmatrix} c \\ c_x \end{bmatrix}^\top \begin{bmatrix} K_{XX} & K_{Xx} \\ K_{xX} & k(x, x) \end{bmatrix}^{-1} \begin{bmatrix} c \\ c_x \end{bmatrix} \leq \Gamma^2 \end{aligned} \quad (6a)$$

$$\|\Lambda c - y\|_{\infty} \leq \bar{\delta} \quad (6b)$$

for any $x \in \Omega \setminus \{X\}$, and extend its value function to points $x = x_i \in X$ with the solution of $\mathbb{P}1' : C(x) = \max_{c \in \mathbb{R}^d} \{c^\top K_{XX}^{-1} c \leq \Gamma^2, \|\Lambda c - y\|_{\infty} \leq \bar{\delta}\}$. The two cases are distinguished since it allows for one decision variable to be eliminated and the quadratic constraint to be simplified. The connection between (5) and (6) is stated next.

Theorem 1. (Finite-dimensional equivalence): *The objective in $\mathbb{P}0$ attains its supremum in \mathcal{H} and $F(x) = C(x)$ for any $x \in \Omega$.*

The derivation of the result follows lines similar to classical representer theorem ones, i.e., showing that the optimizer necessarily lies in a finite-dimensional subspace of the RKHS. Nevertheless, note that the objective $\mathbb{P}1$ is not regularized, nor is x necessarily an input of our dataset. Moreover, the proof given next also establishes the attainment property in \mathcal{H} , which helps in understanding the nature of the constraints.

Proof. Let $\mathbb{X} := X \cup \{x\}$ and define the finite-dimensional subspace $\mathcal{H}^{\parallel} = \{f \in \mathcal{H} : f \in \text{span}(k(x_i, \cdot), x_i \in \mathbb{X})\}$. Furthermore, let $\mathcal{H}^{\perp} = \{g \in \mathcal{H} : \langle g, f^{\parallel} \rangle_{\mathcal{H}} = 0, \forall f^{\parallel} \in \mathcal{H}^{\parallel}\}$ be the orthogonal complement of \mathcal{H}^{\parallel} . Then, we have $\mathcal{H} = \mathcal{H}^{\parallel} \oplus \mathcal{H}^{\perp}$ and for all $f \in \mathcal{H}$, $\exists f^{\parallel} \in \mathcal{H}^{\parallel}, f^{\perp} \in \mathcal{H}^{\perp} : f = f^{\parallel} + f^{\perp}$. By employing the latter decomposition and using the reproducing property, we can reformulate P0 in terms of \mathcal{H}^{\parallel} and \mathcal{H}^{\perp} as

$$\sup_{\substack{f^{\parallel} \in \mathcal{H}^{\parallel} \\ f^{\perp} \in \mathcal{H}^{\perp}}} \{ \langle f^{\parallel} + f^{\perp}, k(x, \cdot) \rangle_{\mathcal{H}} : \|f^{\parallel} + f^{\perp}\|_{\mathcal{H}}^2 \leq \Gamma^2, \|(f^{\parallel} + f^{\perp})_X - y\|_{\infty} \leq \bar{\delta} \} \quad (7)$$

$$\stackrel{(i)}{=} \sup_{\substack{f^{\parallel} \in \mathcal{H}^{\parallel} \\ f^{\perp} \in \mathcal{H}^{\perp}}} \{ f^{\parallel}(x) : \|f^{\parallel}\|_{\mathcal{H}}^2 + \|f^{\perp}\|_{\mathcal{H}}^2 \leq \Gamma^2, \|f_X^{\parallel} - y\|_{\infty} \leq \bar{\delta} \} \quad (8)$$

$$\stackrel{(ii)}{=} \sup_{f^{\parallel} \in \mathcal{H}^{\parallel}} \{ f^{\parallel}(x) : \|f^{\parallel}\|_{\mathcal{H}}^2 \leq \Gamma^2, \|f_X^{\parallel} - y\|_{\infty} \leq \bar{\delta} \} \quad (9)$$

In (i), the f^{\perp} component vanished from the cost and from the last constraint due to orthogonality w.r.t. $k(x_i, \cdot) \in \mathcal{H}^{\parallel}$ for any $x_i \in \mathbb{X}$; moreover, the Pythagorean relation $\|f\|_{\mathcal{H}}^2 = \|f^{\parallel}\|_{\mathcal{H}}^2 + \|f^{\perp}\|_{\mathcal{H}}^2$ was also used. To arrive at the second equality (ii), one only has to note that the objective is insensitive to f^{\perp} and that any $f^{\perp} \neq 0_{\mathcal{H}}$ would tighten the first constraint.

The attainment of the supremum is addressed next. Consider (9) and denote the members of \mathcal{H}^{\parallel} simply as f . $\|f\|_{\mathcal{H}}^2 \leq \Gamma^2$ is a closed and bounded constraint as it is the sublevel set of a norm. We transform $\|f_X - y\|_{\infty} \leq \bar{\delta}$ into $|f(x_i) - y_{i,j}| \leq \bar{\delta}$, $i = 1, \dots, d$, $j = 1, \dots, n_i$. Sets of the form $\{a \in \mathbb{R} : |a| \leq b\}$ are clearly closed in \mathbb{R} , hence $\{f(x_i) \in \mathbb{R} : |f(x_i) - y_{i,j}| \leq \bar{\delta}, \forall i, j\}$ is also closed. For any x_i , the evaluation functional $L_{x_i}(f) = f(x_i)$ is a linear operator and thus pre-images of closed sets are also closed. Consequently, $\{f \in \mathcal{H}^{\parallel} : |f(x_i) - y_{i,j}| \leq \bar{\delta}, \forall i, j\}$ is closed in \mathcal{H}^{\parallel} . The intersection of a finite number of closed sets is necessarily closed, thus all constraint present in (9) define a closed feasible set. Since \mathcal{H}^{\parallel} is finite-dimensional, any closed and bounded subset of it is compact (Heine–Borel); therefore, the continuous objective $L_x(f) = f(x)$ in (9) attains a maximum by the Weierstrass extreme value theorem.

Finally, we establish the connection between P0 and P1. From the above arguments, an optimizer for P0 must lie in \mathcal{H}^{\parallel} . The members $f \in \mathcal{H}^{\parallel}$ have the form $f(z) = \alpha^T K_{Xz}$, being defined by the α weights. Due to the positive-definiteness of k , there exists a bijective map between outputs at the \mathbb{X} locations $f_{\mathbb{X}} = [f(x_1) \dots f(x_d) f(x)]^T$ and the weights α , namely $\alpha = K^{-1} f_{\mathbb{X}}$. K denotes the kernel matrix associated with the set $\mathbb{X} = X \cup \{x\}$. Consequently, optimizing over $f \in \mathcal{H}^{\parallel}$ is equivalent to optimizing over $[f(x_1) \dots f(x_d) f(x)]^T =: [c^T \ c_x]^T$. The bounded norm condition can be recast as $\|f\|_{\mathcal{H}}^2 = \langle f, f \rangle_{\mathcal{H}} = \alpha^T K \alpha = [c^T \ c_x]^T K^{-1} [c^T \ c_x]^T$. The remaining constraint and the objective are straightforward. Noting that this reformulation is valid for any $x \in \Omega$ concludes the proof. \square

Complementing (5), one could also be interested in the infimum $\inf_{f \in \mathcal{H}} \{f(x) : \|f\|_{\mathcal{H}} \leq \Gamma, \|f_X - y\|_{\infty} \leq \bar{\delta}\}$ bounding the lowest attainable value at x . In this case, a result analogous to Theorem 1 could be established, showing its equivalence to

$$\begin{aligned} B(x) &= \min_{c \in \mathbb{R}^d, c_x \in \mathbb{R}} \quad c_x \\ \text{subj. to} \quad & \begin{bmatrix} c \\ c_x \end{bmatrix}^T \begin{bmatrix} K_{XX} & K_{Xx} \\ K_{xX} & k(x, x) \end{bmatrix}^{-1} \begin{bmatrix} c \\ c_x \end{bmatrix} \leq \Gamma^2 \end{aligned} \quad (10a)$$

$$\|\Lambda c - y\|_{\infty} \leq \bar{\delta} \quad (10b)$$

for any $x \in \Omega \setminus X$, and extended to $B(x) = \min_{c \in \mathbb{R}^d} \{c^T K_{XX}^{-1} c \leq \Gamma^2, \|\Lambda c - y\|_{\infty} \leq \bar{\delta}\}$ for $x = x_i \in X$. As a result of this subsection, for any point in the domain $x \in \Omega$, the solutions to the two convex programs (6) and (10) define an *uncertainty envelope* that confines the ground-truth to its interior $B(x) \leq f^*(x) \leq C(x)$.

3.1 Width and width shrinkage

Given our knowledge on the noise influence $\bar{\delta}$, it is natural to ask what the limits of the uncertainty quantification technique considered herein are. For example, is the width of the envelope $C(x) - B(x)$ restricted to a certain minimum value that cannot be reduced even with the addition of new data? From (6b), it is clear that at any input location $x_i \in X$, $C(x_i)$ and $B(x_i)$ cannot be more than $2\bar{\delta}$ apart. In addition to that, the presence of the complexity constraint (6a) can bring the two values closer to each other. Depending on how restrictive this latter constraint is for a given x_i , the corresponding output y_i might lie outside the interval between $C(x_i)$ and $B(x_i)$. In this case, the resulting width is considerably reduced as illustrated in Figure 1 (left).

Proposition 1. (Width smaller than the noise bound): *If $\exists y_i$ such that $y_{i,j} > C(x_i)$ or $y_{i,j} < B(x_i)$ for some j , then $C(x_i) - B(x_i) \leq \bar{\delta}$.*

Proof. Follows from $C(x_i) \geq B(x_i)$, $C(x_i) \leq y_{i,j} + \bar{\delta}$ and $B(x_i) \geq y_{i,j} - \bar{\delta}$ for any $i = 1, \dots, d$ and any $j = 1, \dots, n_i$. \square

Suppose now one has sampled (x_i, y_i) with $y_i = [y_{i,1} \ y_{i,2}]^\top$, $y_{i,1} = f^*(x_i) + \bar{\delta}$ and $y_{i,2} = f^*(x_i) - \bar{\delta}$. Then there is no uncertainty whatsoever about f^* at x_i since $f^*(x_i) = (y_{i,1} + y_{i,2})/2$ is the only possible value attainable by the ground-truth. This illustrates that the possibility of having multiple outputs at the same location allows for the uncertainty interval to shrink past the $\bar{\delta}$ width, and eventually even reduce to a singleton as shown in Figure 1 (right). Notwithstanding, the addition of a new datum to an existing dataset—be it in the form of a new output at an already sampled location or a completely new input-output pair—can only reduce the uncertainty.

Proposition 2. (Decreasing uncertainty): *Let $C_1(x)$ denote the solution of $\mathbb{P}1$ with a dataset $D_1 = \{(x_i, y_i)\}_{i=1}^d$, and $C_2(x)$ the solution with $D_2 = D_1 \cup \{(x_{d+1}, y_{d+1})\}$. Then $C_2(x) \leq C_1(x)$ for any $x \in \Omega$.*

Proof. Denote by $\mathbb{P}1_1$ the problem solved with D_1 and decision variables $[c \ c_x]$. Similarly, $\mathbb{P}1_2$ is associated with the dataset D_2 and the decision variables $[c \ c_x \ c_z]$, where c_z are due to the additional input in D_2 . Since D_2 contains all members of D_1 , the ∞ -norm constraint of $\mathbb{P}1_2$ can be recast as that of $\mathbb{P}1_1$ and an additional constraint for c_z and the new outputs. Let $\bar{X} := X \cup \{x\}$, $\bar{c} := [c^\top \ c_x]^\top$ and $z := x_{d+1}$ be shorthand variables to ease notation. The complexity constraint of $\mathbb{P}1_2$ is then

$$\begin{bmatrix} \bar{c} \\ c_z \end{bmatrix}^\top \begin{bmatrix} K_{\bar{X}\bar{X}} & K_{\bar{X}z} \\ K_{z\bar{X}} & k(z, z) \end{bmatrix}^{-1} \begin{bmatrix} \bar{c} \\ c_z \end{bmatrix} \leq \Gamma^2 \quad (11a)$$

$$\stackrel{(i)}{\Leftrightarrow} \bar{c}^\top K_{\bar{X}\bar{X}}^{-1} \bar{c} + P_{\bar{X}}^{-2}(z) \begin{bmatrix} \bar{c} \\ c_z \end{bmatrix}^\top \begin{bmatrix} K_{\bar{X}\bar{X}}^{-1} K_{\bar{X}z} \\ -1 \end{bmatrix} \begin{bmatrix} K_{\bar{X}\bar{X}}^{-1} K_{\bar{X}z} \\ -1 \end{bmatrix} \begin{bmatrix} \bar{c} \\ c_z \end{bmatrix} \leq \Gamma^2 \quad (11b)$$

$$\stackrel{(ii)}{\Leftrightarrow} \begin{bmatrix} c \\ c_x \end{bmatrix}^\top \begin{bmatrix} K_{XX} & K_{Xx} \\ K_{xX} & k(x, x) \end{bmatrix}^{-1} \begin{bmatrix} c \\ c_x \end{bmatrix} + P_{\bar{X}}^{-2}(z) (\bar{c}^\top K_{\bar{X}\bar{X}}^{-1} K_{\bar{X}z} - c_z)^2 \leq \Gamma^2 \quad (11c)$$

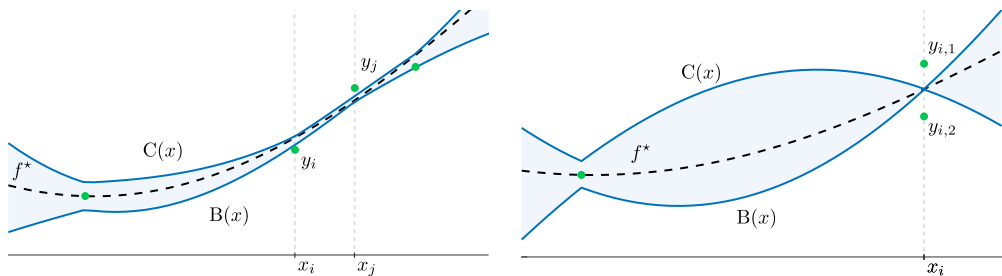


Figure 1: (Left) Samples lying outside of the uncertainty envelope, implying that the width is smaller than the noise bound at x_i and x_j . (Right) A situation where redundant information is used to shrink the uncertainty envelope. In this scenario, we recover the ground-truth value at x_i as $C(x_i) = B(x_i) = f^*(x_i)$.

where the matrix identity found in Appendix E was used in (i) and $P_{\bar{X}}^2(z) = k(z, z) - K_{z\bar{X}}K_{\bar{X}\bar{X}}^{-1}K_{\bar{X}z}$. In (ii), the definitions of \bar{c} and \bar{X} were used. Thanks to $P_{\bar{X}}(z) \geq 0, \forall z$ and the quadratic term multiplying it, we conclude that for any choice of the decision variable c_z , (11c) is a tightened version of the complexity constraint of $\mathbb{P}1_1$, which is (6a). As a result, the maximum of $\mathbb{P}1_2$ is lower or equal than that of $\mathbb{P}1_1$. \square

Let us take a closer look at the tightened constraint (11c). The term $\bar{c}^\top K_{\bar{X}\bar{X}}^{-1}K_{\bar{X}z} =: s(z)$ represents an interpolating model passing through the output values \bar{c} , that is, c and c_x (see e.g. the discussion in Section 3.1 of [Maddalena et al., 2020b]). If the difference $s(z) - c_z$ can be made small, then the tightening will also be reduced, whereas it will be significant if the difference is large. The result is of course dictated by the ∞ -norm constraint since c_z cannot be more than $\bar{\delta}$ away from all the outputs y available at z . Therefore, a new datum will cause significant shrinkage of the envelope at a point $z \in \Omega$ when the new output causes $s(z) - c_z$ to be large. Finally, this process is weighted by the inverse of the power function $P_{\bar{X}}^{-2}(z)$, which does not depend on any output, but only on the input locations.

Remark 2. Recovering the ground-truth as shown in Figure 1 (right) requires the noise realizations to match $\bar{\delta}$ and $-\bar{\delta}$; it is thus necessary to have tight noise bounds for it to happen. On the other hand, Proposition 2 guarantees the decreasing uncertainty property regardless of how precise $\bar{\delta}$ is. Although not explicitly stated, a completely analogous result holds for the lower part of the envelope $B(x)$.

3.2 Sub-optimal closed-form alternatives

The discussion in this subsection assumes that only one sample is present at each input location, i.e., $y_i = y_i$ for $i = 1, \dots, d$, so that $y = y$.

In order to alleviate the computational complexity of having to solve two optimization problems at each query point, closed-form expressions can be employed to compute upper and lower uncertainty estimates. These surrogates yield suboptimal bounds, and can be established around *any* kernel model $s \in \mathcal{H}$, $s(x) = \alpha^\top K_{Xx}$, $\alpha \in \mathbb{R}^d$ as stated next.

Proposition 3. *Let $s(x) = \alpha^\top K_{Xx}$, $\alpha \in \mathbb{R}^d$ be an arbitrary kernel model. For any point $x \in \Omega$, the ground-truth is bounded by $s(x) - S(x) \leq f^*(x) \leq s(x) + S(x)$ with*

$$S(x) = P_X(x) \sqrt{\Gamma^2 + \tilde{\Delta}} + \bar{\delta} \|K_{XX}^{-1}K_{Xx}\|_1 + |\tilde{s}(x) - s(x)| \quad (12)$$

where $\tilde{s}(x) = y^\top K_{XX}^{-1}K_{Xx}$, and the constant $\tilde{\Delta} \in \mathbb{R}$ is the solution of the unconstrained convex problem $\min_{\nu \in \mathbb{R}^d} \left\{ \frac{1}{4} \nu^\top K_{XX} \nu + \nu^\top y + \bar{\delta} \|\nu\|_1 \right\}$.

Proof. See Appendix C.

The map $\tilde{s}(x) = y^\top K_{XX}^{-1}K_{Xx}$ is an interpolant for the available outputs y . Note also that none of the terms in (12) depend on the model weights α with the exception of the last term $|\tilde{s}(x) - s(x)|$. Therefore, the width $S(x)$ will be minimized when $s(x) = \tilde{s}(x) \implies \alpha = y^\top K_{XX}^{-1}$. Since such a model would severely overfit, a balance between smoothing the data and not diverging too much from $\tilde{s}(x)$ has to be found. In our previous work [Maddalena et al., 2020b], we have illustrated how kernel ridge regression and minimum norm models are good candidate techniques to accomplish this goal.

By reformulating the optimal bounds, we uncover their relation with the suboptimal estimates given in Proposition 3. First, consider $\mathbb{P}1$ and optimize over the decision variable $\delta = c - y$ rather than over c . Next, apply a quadratic decomposition identical to the one used in (11) to the complexity constraint (6a) and solve for c_x . After recalling that $\tilde{s}(x) = y^\top K_{XX}^{-1}K_{Xx}$ and $\|\tilde{s}\|_{\mathcal{H}}^2 = y^\top K_{XX}^{-1}y$, one obtains

$$c_x \leq \tilde{s}(x) + P(x) \sqrt{\Gamma^2 - \|\tilde{s}\|_{\mathcal{H}}^2 - \delta^\top K_{XX}^{-1}\delta + 2y^\top K_{XX}^{-1}\delta + \delta^\top K_{XX}^{-1}K_{Xx}} \quad (13)$$

Instead of maximizing c_x , the right-hand side of (13) can be directly considered as the objective function equivalently. As a result, we obtain $\max_{\delta \in \mathbb{R}^d} \{\tilde{s}(x) + P(x) \sqrt{\Gamma^2 - \|\tilde{s}\|_{\mathcal{H}}^2 - \delta^\top K_{XX}^{-1} \delta - 2y^\top K_{XX}^{-1} \delta + \delta^\top K_{XX}^{-1} K_{Xx}} : \|\delta\|_\infty \leq \bar{\delta}\}$. Now, relax the problem by allowing δ to attain different values inside and outside the square-root

$$\max_{\delta_1, \delta_2 \in \mathbb{R}^d} \tilde{s}(x) + P(x) \sqrt{\Gamma^2 - \|\tilde{s}\|_{\mathcal{H}}^2 - \delta_1^\top K_{XX}^{-1} \delta_1 + 2y^\top K_{XX}^{-1} \delta_1 + \delta_2^\top K_{XX}^{-1} K_{Xx}} \quad (14a)$$

$$\text{subj. to } \|\delta_1\|_\infty \leq \bar{\delta}, \|\delta_2\|_\infty \leq \bar{\delta} \quad (14b)$$

Note that the objective is separable and that $\tilde{\Delta}$ is the dual solution of $\max_{\delta_1 \in \mathbb{R}^d} \{\delta_1^\top K_{XX}^{-1} \delta_1 - 2y^\top K_{XX}^{-1} \delta_1 + \|\tilde{s}\|_{\mathcal{H}}^2\}$. Also, $\max_{\delta_2 \in \mathbb{R}^d} \{\delta_2^\top K_{XX}^{-1} K_{Xx} : \|\delta_2\|_\infty \leq \bar{\delta}\} = \bar{\delta} \|K_{XX}^{-1} K_{Xx}\|_1$ since these norms are duals of each other. Remember that the objective (14a) is a conservative upper bound for $f^*(x)$, having $\tilde{s}(x)$ as the reference model. Given any smoother $s(x)$, the triangle inequality $|f(x) - s(x)| \leq |f(x) - \tilde{s}(x)| + |\tilde{s}(x) - s(x)|$ can be used to bound the distance between its predictions and the ground-truth values, arriving thus at the same expressions presented in Proposition 3.

From (13), the noise variable δ is seen to increase the maximum in two distinct ways: through the inner product $\delta^\top K_{XX}^{-1} K_{Xx}$, and via a norm augmentation corresponding to $\tilde{\Delta}$. One source of conservativeness in Proposition 3 is taking into account the worst-possible inner-product and norm increase jointly. Despite this fact, they yield competitive results for moderate noise-levels. We moreover note that in the noise-free scenario, (13) and (14a) are the same, and Proposition 3 simplifies to the classical bounds in the interpolation case (see for instance [Fasshauer, 2011]).

Remark 3. The closed-form bounds presented in this subsection feature nominal models as their center, which is desirable in many practical situations. In the optimal scenario, the minimum norm regressor $s^*(x) = \alpha^{*\top} K_{Xx}$, $\alpha^* = \arg \min_{\alpha \in \mathbb{R}^d} \{\alpha^\top K_{XX} \alpha : \|K_{XX} \alpha - y\|_\infty \leq \bar{\delta}\}$ can be used as a nominal model. This choice is guaranteed to lie completely within $C(x)$ and $B(x)$ —although not necessarily in the middle—since the map s^* belongs to \mathcal{H} and is a feasible solution for P0.

4 Efficient computation and outer approximations

One of the fundamental sources of computational complexity in kernel learning lies in the inverse term K_{XX}^{-1} . Scaling these techniques to large datasets in a principled manner is still a topic of active research [Zhang et al., 2013, Burt et al., 2020]. Notice that K_{XX}^{-1} is explicitly present in P1, thus limiting its applicability to small and medium-sized problems due to the cubic time complexity associated with the inverse operation. In this section we discuss alternative formulations that can be solved more efficiently.

4.1 The dual problem

Following a standard dualization procedure, which can be found in Appendix D, a Lagrangian dual for P1 in (6) can be the convex problem D1

$$\min_{\nu \in \mathbb{R}^d, \lambda > 0} \frac{1}{4\lambda} \nu^\top \Lambda K_{XX} \Lambda^\top \nu + \left(y - \frac{1}{2\lambda} \Lambda K_{Xx} \right)^\top \nu + \bar{\delta} \|\nu\|_1 + \frac{1}{4\lambda} k(x, x) + \lambda \Gamma^2 \quad (15)$$

for any query point $x \in \Omega \setminus X$. In our notation the dimension $\tilde{d} = \sum_{i=1}^d n_i$ is the total number of outputs, that is, the size of y . As detailed in Appendix D, under the assumption of the complexity constrain not being active, the dual of P1' is also D1, meaning that the formulation (15) could be used $\forall x \in \Omega$.

Remarkably, $\mathbb{D}1$ only involves the kernel matrix itself and not its inverse, avoiding thus the aforementioned adversity. Furthermore, the query point x enters $\mathbb{D}1$ through the terms K_{Xx} and $k(x, x)$. The former measures the similarity between the query point x and each of the inputs in X ; the latter is simply a constant term for translation-invariant kernels, and evaluates always to 1 in the specific case of the squared-exponential kernel.

The optimization problem above is convex since it is a quadratic-over-linear function with $\Lambda K_{XX} \Lambda^\top \succeq 0$ and λ restricted to the positive reals. The objective can moreover be decomposed into a differentiable part and a single non-differentiable term $\|\nu\|_1$, with ν unconstrained. This class of problems has long been studied and mature numerical algorithms exist to solve them, notably different flavors of splitting methods such as the alternating direction method of multipliers (ADMM) [Boyd et al., 2011, Section 6]. Alternatively, a standard linear reformulation could be employed to substitute $\|\nu\|_1$ by $\sum_i \eta_i$, with additional constraints $-\nu \leq \eta, \nu \leq \eta$. The result is a completely differentiable objective, but with extra decision variables and linear constraints. Next, a mild condition is given ensuring a zero duality gap between the primal and dual problems.

Proposition 4. (Strong duality): *If $\bar{\delta} > \delta_{i,j}, \forall i, j$ and $\Gamma > \|f^*\|_{\mathcal{H}}$, then no duality gap exists, i.e., $\max \mathbb{P}1 = \min \mathbb{D}1$.*

Proof. Consider the primal problem $\mathbb{P}1$ and select $c = f_X^*$ and $c_x = f^*(x)$. Let $\mathbb{X} := X \cup \{x\}$ and $\mathbb{K}(x)$ denote the kernel matrix associated with \mathbb{X} . Thanks to the optimal recovery property [Wendland, 2004, Theorem 13.2], $[c^\top \ c_x] \mathbb{K}(x) [c^\top \ c_x]^\top \leq \|f^*\|_{\mathcal{H}}^2$, which in turn is strictly smaller than Γ^2 by assumption. Also, $\|\Lambda c - y\|_\infty = \|\Lambda f_X^* - y\|_\infty = \|[\delta_{1,1} \ \dots \ \delta_{2,1} \ \dots]^\top\|_\infty < \bar{\delta}$. Therefore, the ground-truth values constitute a feasible solution that lies in the interior of the primal problem feasible set. As a result, Slater's condition is met and, since the primal is convex, there is no duality gap. \square

4.2 An alternating optimization procedure

Solving the dual problem to any accuracy leads to an over bound on $C(x)$ thanks to duality. In other words, any feasible sub-optimal solution of $\mathbb{D}1$ establishes a conservative uncertainty estimate. This motivates the study of light methods that could trade-off computational time and accuracy. In what follows we describe a block coordinate minimization scheme to tackle the problem, which is later shown to yield reasonable results after only a small number of iterations.

Whenever λ is fixed to a particular positive value $\lambda^* > 0$, the problem (15) simplifies to an unconstrained quadratic program (QP) in ν of the form $\min_{\nu \in \mathbb{R}^{\tilde{d}}} \tilde{C}_x(\lambda^*, \nu)$. On the other hand, if ν is fixed to $\nu^* \in \mathbb{R}^{\tilde{d}}$, the dual objective takes the form

$$\min_{\lambda \in \mathbb{R}_{>0}} \tilde{C}_x(\lambda, \nu^*) = \min_{\lambda \in \mathbb{R}_{>0}} \frac{c_1}{\lambda} + c_2 \lambda + c_3 \quad (16)$$

with the constants

$$c_1 = \frac{1}{4} \begin{bmatrix} \Lambda^\top \nu^* \\ -1 \end{bmatrix}^\top \mathbb{K}(x) \begin{bmatrix} \Lambda^\top \nu^* \\ -1 \end{bmatrix}, \quad c_2 = \Gamma^2, \quad c_3 = y^\top \nu^* + \bar{\delta} \|\nu^*\|_1 \quad (17)$$

and $\mathbb{K}(x) \succeq 0$. We have $\frac{\partial \tilde{C}_x(\lambda, \nu^*)}{\partial \lambda} = \frac{-c_1}{\lambda^2} + c_2$ which gives the candidate solution $\lambda^* = \sqrt{c_1/c_2}$ for (16). We have $c_2 > 0$ and $c_1 \geq 0$ for any $x \in \Omega$, and $c_1 > 0$ for any $x \in \Omega \setminus X$. Furthermore, λ^* is indeed a minimizer of (16) for $x \in \Omega \setminus X$ since its curvature is positive, i.e., $\frac{\partial^2 \tilde{C}_x(\lambda^*, \nu^*)}{\partial \lambda^2} > 0$. In closed-form, λ^* takes the following form.

$$\lambda^* = \frac{\sqrt{\nu^{*\top} \Lambda K_{XX} \Lambda^\top \nu^* - 2(\Lambda K_{Xx})^\top \nu^* + k(x, x)}}{2\Gamma} \quad (18)$$

Note that $\lambda^* = 0$ is only possible if $\begin{bmatrix} \Lambda^\top \nu^* \\ -1 \end{bmatrix}$ is in the nullspace of matrix $\mathbb{K}(x)$, which is only possible if $x \in X$. In this case, after fixing $\lambda^* = 0$, the problem to solve for ν reduces to

$$\min_{\nu} \mathbf{y}^\top \nu + \bar{\delta} \|\nu\|_1 \quad \text{s.t.} \quad \begin{bmatrix} \Lambda^\top \nu \\ -1 \end{bmatrix} \in N(\mathbb{K}(x)).$$

We formulate the alternating optimization algorithm for a maximum number of iterations L and a termination threshold ϵ in the following way.

Algorithm 1: Alternating minimization

Result: Upper bound $\tilde{C}(x)$ of the ground-truth at point x
Input: $x, \lambda_0, L, \epsilon$
 $\lambda_0^* = \lambda_0$
 $k = 0$
do

$$\left| \begin{array}{l} \nu^* = \arg \min_{\nu \in \mathbb{R}^{\tilde{d}}} \tilde{C}_x(\lambda_k^*, \nu) \\ \lambda_{k+1}^* = \frac{\sqrt{\nu^{*\top} \Lambda K_{XX} \Lambda^\top \nu^* - 2(\Lambda K_{Xx})^\top \nu^* + k(x, x)}}{2\Gamma} \\ k = k + 1 \end{array} \right.$$

while $k < L$ and $|\lambda_k^* - \lambda_{k-1}^*| > \epsilon$;
 $\tilde{C}(x) = \tilde{C}_x(\lambda_k^*, \nu^*)$

Remark 4. (Numerical properties): Recall the convex dual objective function (15). Since the non-differentiable term $\|\nu\|_1$ is separable and the remainder of the objective is differentiable, a tuple (ν^*, λ^*) that simultaneously minimizes both sub-problems also necessarily minimizes the whole objective (15). For non-asymptotic sublinear convergence rates of alternating minimization algorithms applied to convex programs, the reader is referred to the work [Beck, 2015].

5 On the connections with Gaussian processes

Before proceeding to a numerical example, we contrast our uncertainty quantification technique with Gaussian processes (GPs) regression. By putting them into perspective, we hope to improve the understanding of the theory developed herein.

In the Bayesian framework of GPs, kernels are used to define the covariance between random variables in the input space Ω [Rasmussen and Williams, 2006]. Deeper links also exist between the Hilbert space associated with such stochastic processes and the RKHS \mathcal{H} corresponding to the same kernel map [Parzen et al., 1961], in that there exists an isometric isomorphism connecting both spaces. Moreover, it is known that even though the mean function of a GP does belong to \mathcal{H} , its sample paths almost surely do not if $\dim(\mathcal{H}) = \infty$. Nonetheless, the same paths can belong to another RKHS—not necessarily the one associated with their kernel—with probability one (see [Kanagawa et al., 2018] for a comprehensive discussion on the topic). The latter phenomenon is known as Driscoll’s zero-one law. Although informative, deriving practical guidelines from these results requires care as intuition might lead to wrong conclusions when examining infinite-dimensional spaces. In particular, it is unclear how restrictive GP hypotheses spaces are when compared to assuming $f^* \in \mathcal{H}$ as done in this work.

The variance around the mean of a GP is a form of uncertainty quantification against point-wise outputs drawn from the same distribution. Note that this variance admits a closed-form expression only when the marginal likelihood is Gaussian, and must be numerically approximated if other noise models are used (e.g. heteroscedastic Gaussian, log-Gaussian, Bernoulli) [Rasmussen and Williams, 2006, Chapter 9]. As opposed to it, uniform error bounds measure the uncertainty with respect to complete functions, i.e., whole sample paths [Srinivas et al., 2012, Lederer et al., 2019]. The noise model

considered in the former work is sub-Gaussian, whereas it is Gaussian in the latter. Whether one should opt for the theory developed herein or for Gaussian processes-based techniques is truly a question of model selection. How could the measurement noise be described in my application, and is Gaussianity a sensible assumption? Furthermore, the final yield should also be taken into account. Do probabilistic inequalities suffice or does my application require deterministic certification? In our view, the deterministic and the stochastic frameworks have their own merits [Kanagawa et al., 2018], and the user should judge which of them is more adequate to tackle the problem at hand.

6 Numerical examples

Consider the function below, which represents the first component update map of a Hénon chaotic attractor with an additional sinusoidal forcing term¹

$$f^*(z_1, z_2) = 1 - az_1^2 + z_2 + b \sin(c z_2) \quad (19)$$

The parameters are $a = 0.8$, $b = 8$ and $c = 0.8$, and its domain is the box $\Omega = [-10 \ 10] \times [-10 \ 10]$. A squared-exponential kernel $k(x, x') = \exp\left(\frac{\|x-x'\|^2}{2\ell^2}\right)$ with $x = [z_1 \ z_2]$ was chosen for our experiments with lengthscale $\ell = 5$, which was empirically estimated by gridding the search-space and performing posterior validation. Γ was obtained through the procedure described in Appendix A with a final value of $\Gamma = 1200$. A total of $d = 100$ samples were collected using two strategies: inputs lying in an equidistant grid, and inputs being drawn randomly from a uniform distribution. Throughout the tests, noise was always sampled uniformly with $\bar{\delta} = 1$ and $\bar{\delta} = 5$.

The obtained optimal upper bound $C(x)$ is displayed in Figure 2 along with the ground-function f^* . Consider the scenario $\bar{\delta} = 1$. Whereas the $C(x)$ surface is overall tight for the grid-based dataset, with an average distance of 3.01 to the latent function, randomized data yielded a less regular bound with an average distance of 8.02. These numbers were increased respectively to 9.57 and 18.97 when the noise levels were risen to $\bar{\delta} = 5$. The plots illustrate the disadvantages of relying on completely randomized input locations, which degraded especially the borders of $C(x)$. On the other extreme, an equidistant grid of points is highly favorable, not only filling the domain well, but also ensuring a minimum *separation distance* so that no two inputs are too close to cause numerical problems when handling the kernel matrix K_{XX} .

Next, $f^*(z_1, z_2)$ was sliced at $z_1 = -7.98$ and the whole envelope optimum $B(x) \leq x \leq C(x)$ was computed. This was compared to the closed-form bounds given in Proposition 3 for a kernel ridge regression (KRR) model with regularization constant of 10^{-4} . The two datasets from the previous experiment with $\bar{\delta} = 1$ were kept and the obtained results are shown in Figure 3. As can be seen from the plots, the KRR estimates were rather conservative compared to the blue envelope in the random case. Under a grid of samples however, the two approaches produced comparable results. Lastly, the alternating procedure described in Section 4.2 was tested. Starting with an initial guess of $\lambda = 10^{-3}$, 5 and 10 iterations of the algorithm were run. The results displayed in Figure 4 indicate that while 5 steps yielded a considerably loose envelope (yellow region), 10 steps sufficed to make the approximate solution and the optimal essentially indistinguishable (compare the magenta and blue bounds). We have experimentally noticed that warm starting λ , perhaps with the optimum value obtained from a nearby query point, reduces the number of iterations required to attain high-quality solutions.

The last numerical experiment involves the ground-truth (19) as an unknown constraint of a static problem. Data-driven optimization with unknown constraints is similar to what one would find for instance in the field of real-time optimization. More specifi-

¹All code is available at <https://gitlab.epfl.ch/scharnho/optimal-bounds>.

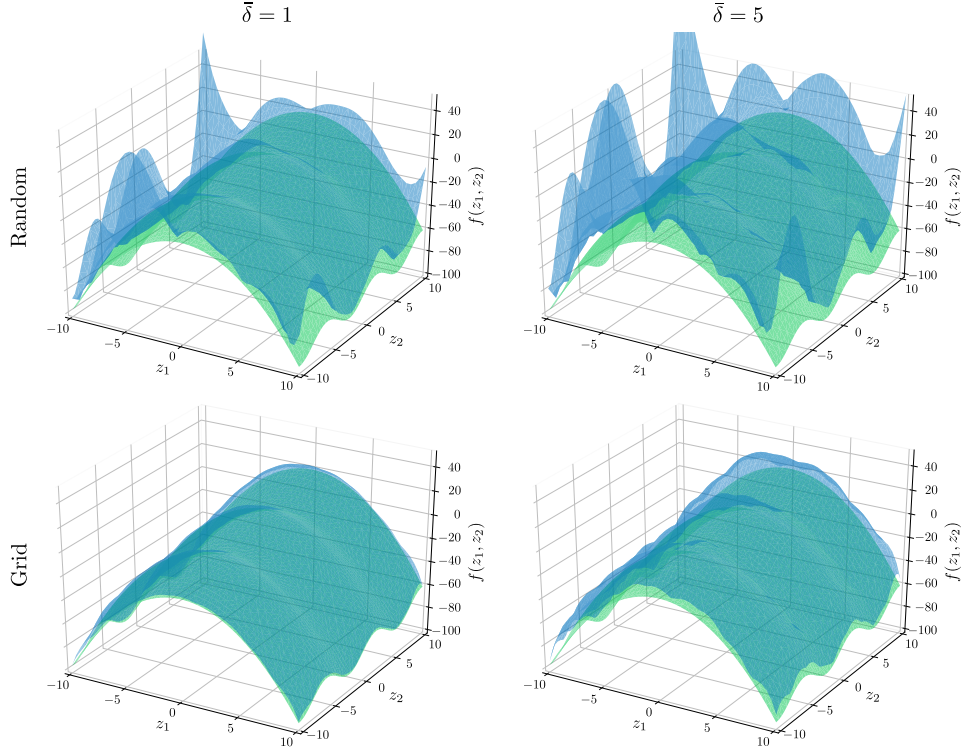


Figure 2: The Hénon chaotic attractor (green) and the upper bound $C(x)$ (blue) after collecting $d = 100$ data-points. Top plots: random samples drawn uniformly. Bottom plots: samples on an equidistant grid. Left plots: $\bar{\delta} = 1$. Right plots: $\bar{\delta} = 5$.

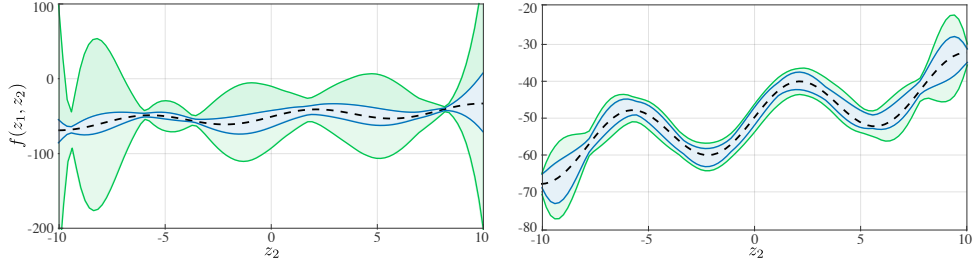


Figure 3: A comparison between the optimal bounds (blue) and the KRR closed-form bounds (green). Left: random samples drawn uniformly. Right: samples on an equidistant grid. The ground-truth was sliced at $z_1 = -7.98$ and is shown in dashed black.

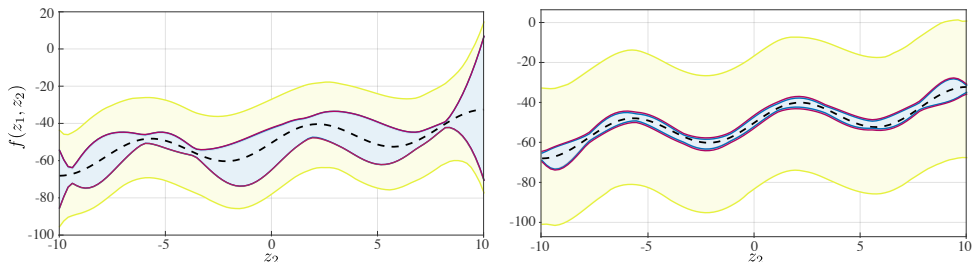


Figure 4: A comparison between the optimal bounds (blue) and the alternating optimization procedure for 5 steps (yellow) and 10 steps (magenta). Left: random samples drawn uniformly. Right: samples on an equidistant grid. The ground-truth was sliced at $z_1 = -7.98$ and is shown in dashed black.

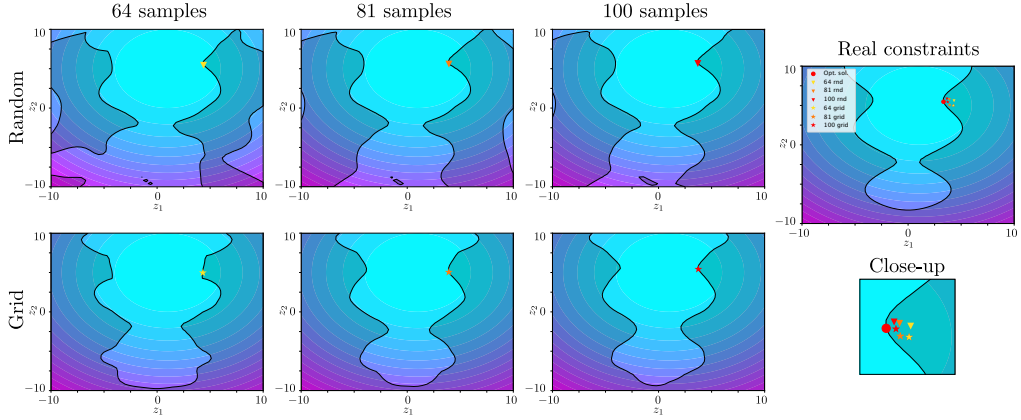


Figure 5: Solutions and feasible sets (shaded areas) for problem (20) with 64, 81 and 100 samples of $g(z)$. Top row: random samples drawn uniformly. Bottom row: samples on an equidistant grid. Rightmost column: the true feasible set and optimal solution.

	64 samples	81 samples	100 samples	Optimal solution
Random	13.216	11.361	10.958	5.691
Grid	10.671	8.477	7.665	

Table 1: Optimal solution and approximate solutions for (20) using the upper bound $C(z)$ as a surrogate for the unknown constraint $g(z)$.

ally, consider the simple formulation

$$\min_{z \in \mathbb{R}^2} (z_1 - 1)^2 + (z_2 - 5)^2 \quad (20a)$$

$$\text{subj. to } g(z) \leq 0 \quad (20b)$$

where $g(z) = f^*(z) + 10$. Samples were used to establish an upper bound $C(z)$ for $g(z)$, hence providing an inner-approximation for the real feasible set. We considered the cases of having 64, 81 and 100 evaluations of $g(z)$ affected by noise with $\bar{\delta} = 1$ and, once more, the data were collected by means of a uniform random distribution and a equidistant grid. In the approximate optimization problems, the original constraint (20b) was replaced by $C(z) \leq 0$. Optimizers z^* were computed by gridding the domain, and the results along with the estimated feasible sets (shaded areas) are shown in Figure 5. Notice how in some instances the set of feasible decisions is not connected. The obtained approximate solutions are listed in Table 1, where the reported random sampling results are the average over 10 dataset realizations. Thanks to Proposition 2, the addition of new data-points can only relax the approximate formulation, explaining the convergence towards the optimal solution shown in Table 1.

7 Final remarks and future directions

We investigated the uncertainty quantification problem associated with evaluations of an unknown function that belongs to a possibly infinite-dimensional reproducing-kernel Hilbert space. Optimal robust bounds were derived by exploiting a finite set of samples and an estimate of the ground-truth function complexity as measured by its norm. Several formulations were then analyzed: a primal finite-dimensional program, one possible dual form, as well as closed-form sub-optimal solutions centered around pre-specified kernel models. When considering the optimal alternatives, it was shown how the addition of new data can only shrink the uncertainty envelope everywhere.

Future research could focus on the following topics. Firstly, the developed theory could be generalized to accept uncertain inputs, thus allowing for uncertainty propagation in multi-stage problems. Additionally, resampling techniques could be used to construct sparse representations or to confer a desired geometrical property on the input points, enabling fast evaluation of the bounds. Finally, the developed finite-sample bounds could give support to the area of data-driven optimization under unknown constraints or objectives by establishing formal feasibility or performance guarantees.

A Estimating RKHS complexity from data

We consider an unknown map $f \in \mathcal{H}$ and a set of samples $D = \{(x_i, f(x_i))\}_{i=1}^d$. Using the shorthand $f_X = [f(x_1) \dots f(x_d)]^\top$, we have that $\hat{\Gamma} := \sqrt{f_X^\top K_{XX}^{-1} f_X} \leq \|f\|_{\mathcal{H}}$ for any number of samples $d \in \mathbb{N}$ due to the optimal recovery property [Wendland, 2004]. Moreover, the decomposition used in the proof of Proposition 2 shows that the quantity $\hat{\Gamma}$ can only increase with the addition of new data. Since $\|f\|_{\mathcal{H}}$ is the least upper bound for it, then this quantity can be used as an efficient lower estimate for the RKHS norm. An example is shown in Figure 6 for an f composed of 25 squared-exponential kernel functions (left). Samples were drawn uniformly and the norm estimates are shown for an increasing number of data (right). The data-points highlighted in green were responsible for over 90% of the final norm estimate. In a practical situation, expert knowledge should be elicited to augment $\hat{\Gamma}$ and transform it into an upper bound $\Gamma \geq \|f\|_{\mathcal{H}}$. Moreover, if the outputs are corrupted by measurement noise, it is possible to quantify its worst-case effect on the estimation process [Maddalena et al., 2020b].

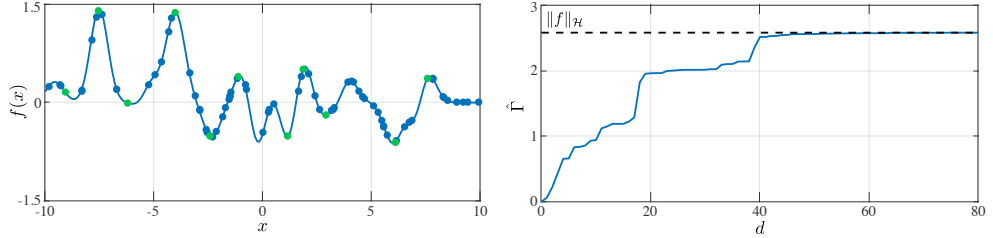


Figure 6: Estimating the RKHS norm using sampled data (all circles). The green samples alone were responsible for more than 90% of the final attained value.

B The data-selection matrix

Recall that n_1, n_2, \dots, n_d are the number of outputs available at the input locations x_1, x_2, \dots, x_d . Λ has size $(\sum_i n_i) \times d$ and is defined as

$$\Lambda := \begin{bmatrix} \mathbf{1}_{n_1} & \mathbf{0}_{n_1} & \mathbf{0}_{n_1} & \cdots & \mathbf{0}_{n_1} \\ \mathbf{0}_{n_2} & \mathbf{1}_{n_2} & \mathbf{0}_{n_2} & \cdots & \mathbf{0}_{n_2} \\ \vdots & \vdots & \vdots & \ddots & \vdots \\ \mathbf{0}_{n_d} & \mathbf{0}_{n_d} & \mathbf{0}_{n_d} & \cdots & \mathbf{1}_{n_d} \end{bmatrix} \quad (21)$$

where $\mathbf{1}_{n_i}$ and $\mathbf{0}_{n_i}$ are respectively column vectors of ones and zeros of size n_i . If only a single output is available at every input, Λ simplifies to an identity matrix.

C Proof of Proposition 3

For any given $s(x) = \alpha^\top K_{Xx}$, we have

$$|f^*(x) - s(x)| = |f^*(x) - \tilde{s}(x) + \tilde{s}(x) - s(x)| \quad (22)$$

$$\leq |f^*(x) - (f_X^* + \delta_X)K_{XX}^{-1}K_{Xx}| + |\tilde{s}(x) - s(x)| \quad (23)$$

$$\leq |f^*(x) - \bar{s}(x)| + \bar{\delta} \|K_{XX}^{-1}K_{Xx}\|_1 + |\tilde{s}(x) - s(x)| \quad (24)$$

$$\leq P(x) \sqrt{\Gamma^2 - \|\bar{s}\|_{\mathcal{H}}^2} + \bar{\delta} \|K_{XX}^{-1}K_{Xx}\|_1 + |\tilde{s}(x) - s(x)| \quad (25)$$

$$\leq P(x) \sqrt{\Gamma^2 + \Delta - \|\tilde{s}\|_{\mathcal{H}}^2} + \bar{\delta} \|K_{XX}^{-1}K_{Xx}\|_1 + |\tilde{s}(x) - s(x)| \quad (26)$$

with f_X^* being the vector of true function values at the sample locations in X and δ_X the vector of additive measurement noise for the samples y . (23) follows from the triangle inequality and the additive noise property of y . Using the triangle inequality again, we arrive at (24), where \bar{s} denotes the noise-free interpolant of f_X^* . The noise-free interpolation error bound gives the estimation in the first term of (25), while (26) follows from [Maddalena et al., 2020b, Lemma 1], with $\Delta = \max_{\|\delta\|_\infty \leq \bar{\delta}} (-\delta^\top K_{XX}^{-1}\delta + 2y^\top K_{XX}^{-1}\delta)$. A standard dualization procedure as the one presented in Appendix D leads to the dual problem

$$\min_{\nu \in \mathbb{R}^d} \frac{1}{4} \nu^\top K_{XX} \nu + \nu^\top y + \bar{\delta} \|\nu\|_1 + y^\top K_{XX}^{-1} y \quad (27)$$

for Δ . Notice that the last term in (27) is constant and the same as the squared interpolant norm $\|\tilde{s}\|_{\mathcal{H}}^2$. Therefore, these terms cancel in (26) and we are left with

$$|f^*(x) - s(x)| \leq P(x) \sqrt{\Gamma^2 + \tilde{\Delta}} + \bar{\delta} \|K_{XX}^{-1}K_{Xx}\|_1 + |\tilde{s}(x) - s(x)| \quad (28)$$

where $\tilde{\Delta}$ represents (27) without the constant term.

D Dual problem derivation

Consider the case $x \notin X$. Let $z := [c^\top \ c_x]^\top$, $a := [\mathbf{0}^\top \ 1]^\top$, $A := [\mathbf{I} \ \mathbf{0}]$. The Lagrangian of P1 is

$$\mathcal{L}(z, \lambda, \beta, \gamma) = a^\top z - \lambda(z^\top \mathbb{K}(x)^{-1}z - \Gamma^2) - \beta^\top (\Lambda Az - y - \bar{\delta}\mathbf{1}) - \gamma^\top (y - \Lambda Az - \bar{\delta}\mathbf{1}) \quad (29)$$

where $\mathbb{K}(x)$ denotes the kernel matrix evaluated at $X \cup \{x\}$. Suppose $\lambda > 0$. Computing $\nabla_z \mathcal{L}(z^*) = 0$ leads to $z^* = -\frac{1}{2\lambda} \mathbb{K}(x) (A^\top \Lambda^\top (\beta - \gamma) - a)$. Defining the auxiliary variable $\nu = \beta - \gamma$, and substituting z^* into (29) gives the dual objective

$$\begin{aligned} g(\lambda, \nu) &= \frac{1}{4\lambda} \nu^\top \Lambda A \mathbb{K}(x) A^\top \Lambda^\top \nu + \left(y - \frac{1}{2\lambda} \Lambda A \mathbb{K}(x) a \right)^\top \nu + \bar{\delta} \|\nu\|_1 + \frac{1}{4\lambda} a^\top \mathbb{K}(x) a + \lambda \Gamma^2 \\ &= \frac{1}{4\lambda} \nu^\top \Lambda K_{XX} \Lambda^\top \nu + \left(y - \frac{1}{2\lambda} \Lambda K_{Xx} \right)^\top \nu + \bar{\delta} \|\nu\|_1 + \frac{1}{4\lambda} k(x, x) + \lambda \Gamma^2 \end{aligned} \quad (30)$$

where in the second equality the matrix $\mathbb{K}(x)$ was expanded and the resulting terms were reorganized. Since $\beta, \gamma \in \mathbb{R}_{\geq 0}^d$ and $\nu = \beta - \gamma$ then ν is unconstrained.

Now if $\lambda = 0$, the Lagrangian (29) simplifies to $\mathcal{L}(z, \nu) = (a - A^\top \Lambda^\top \nu)^\top z + \nu^\top y + \bar{\delta} \|\nu\|_1$, which is linear in z . Its supremum w.r.t. z is only finite if $a = A^\top \Lambda^\top \nu$. Recalling the definitions of a , A and Λ , one can see that ν that could satisfy the latter condition. Therefore, $\lambda = 0 \implies \sup_z \mathcal{L}(z, \lambda, \nu) = +\infty$, meaning that the dual problem is infeasible. As a conclusion, the Lagrangian dual of P1 in (6) is precisely D1 in (15).

Next, consider the case $x \in X$, $x = x_i$. The objective of $\mathbb{P}1'$ can be written as $a^\top c$ with $a_i = 1$ and $a_n = 0, n \neq i$. When deriving its Lagrangian, one obtains again (29) with the simplifications: $z \leftarrow c$, $\mathbb{K}(x) \leftarrow K_{XX}$ and $A \leftarrow \mathbf{I}$. We proceed by analyzing the two scenarios for λ as before. If $\lambda > 0$, the previous derivations apply, leading to the same quadratic-over-linear objective (30). However, if $\lambda = 0$, the Lagrangian becomes $\mathcal{L}(z, \nu) = (a - \Lambda^\top \nu)^\top z + \nu^\top y + \bar{\delta} \|\nu\|_1$, whose supremum w.r.t. z is only finite if $a = \Lambda^\top \nu$. In contrast with the previous paragraph, this condition now can be satisfied. It is equivalent to $\nu_{i,1} + \dots + \nu_{i,n_i} = 1$, where the variables are all the multipliers associated with the i -th input location x_i . The resulting expression can be minimized analytically, yielding the minimum $\min_j y_{i,j} + \bar{\delta}$, i.e., the smallest output available at x_i augmented by the noise bound. Finally, we conclude that the dual objective for $\mathbb{P}1'$ is

$$g(\lambda, \nu) = \begin{cases} (30), & \text{if } \lambda > 0 \\ \min_j y_{i,j} + \bar{\delta}, & \text{if } \lambda = 0 \end{cases} \quad (31)$$

As a last observation, a dual problem can also be derived for (10), calculating the lower part of the envelope. The formulation is analogous to (15), assuming the form

$$\max_{\nu \in \mathbb{R}^d, \lambda > 0} -\frac{1}{4\lambda} \nu^\top \Lambda K_{XX} \Lambda^\top \nu - \left(y + \frac{1}{2\lambda} \Lambda K_{Xx} \right)^\top \nu - \bar{\delta} \|\nu\|_1 - \frac{1}{4\lambda} k(x, x) - \lambda \Gamma^2 \quad (32)$$

Note that these are distinct objectives, not merely opposites. Therefore, two problems have to be solved to fully quantify the ground-truth uncertainty.

E A block matrix identity

Let $A \in \mathbb{R}^{d \times d}$ be invertible, $B \in \mathbb{R}^d$ and $c \in \mathbb{R}$. The following identity holds

$$\begin{bmatrix} A & B \\ B^\top & c \end{bmatrix}^{-1} = \begin{bmatrix} A^{-1} + \frac{1}{d} A^{-1} B B^\top A^{-1} & -\frac{1}{d} A^{-1} B \\ -\frac{1}{d} B^\top A^{-1} & \frac{1}{d} \end{bmatrix} \quad (33)$$

where $d = c - B^\top A^{-1} B$.

Acknowledgment

This work has received support from the Swiss National Science Foundation under the RISK project (Risk Aware Data-Driven Demand Response, grant number 200021 175627).

References

- [Beck, 2015] Beck, A. (2015). On the convergence of alternating minimization for convex programming with applications to iteratively reweighted least squares and decomposition schemes. *SIAM Journal on Optimization*, 25(1):185–209.
- [Belkin, 2018] Belkin, M. (2018). Approximation beats concentration? an approximation view on inference with smooth radial kernels. In *Conference On Learning Theory*, pages 1348–1361. PMLR.
- [Berkenkamp et al., 2016] Berkenkamp, F., Schoellig, A. P., and Krause, A. (2016). Safe controller optimization for quadrotors with gaussian processes. In *2016 IEEE International Conference on Robotics and Automation (ICRA)*, pages 491–496. IEEE.

[Bertsimas and Koduri, 2021] Bertsimas, D. and Koduri, N. (2021). Data-driven optimization: A reproducing kernel hilbert space approach. *Operations Research*.

[Boyd et al., 2011] Boyd, S., Parikh, N., and Chu, E. (2011). *Distributed optimization and statistical learning via the alternating direction method of multipliers*. Now Publishers Inc.

[Burt et al., 2020] Burt, D. R., Rasmussen, C. E., and van der Wilk, M. (2020). Convergence of sparse variational inference in gaussian processes regression. *Journal of Machine Learning Research*, 21:1–63.

[Chakrabarty et al., 2016] Chakrabarty, A., Dinh, V., Corless, M. J., Rundell, A. E., Źak, S. H., and Buzzard, G. T. (2016). Support vector machine informed explicit nonlinear model predictive control using low-discrepancy sequences. *IEEE Transactions on Automatic Control*, 62(1):135–148.

[Chen et al., 2014] Chen, T., Andersen, M. S., Ljung, L., Chiuso, A., and Pillonetto, G. (2014). System identification via sparse multiple kernel-based regularization using sequential convex optimization techniques. *IEEE Transactions on Automatic Control*, 59(11):2933–2945.

[Cucker and Zhou, 2007] Cucker, F. and Zhou, D. X. (2007). *Learning theory: An approximation theory viewpoint*, volume 24. Cambridge University Press.

[De Matthews et al., 2018] De Matthews, A., Hron, J., Rowland, M., Turner, R., and Ghahramani, Z. (2018). Gaussian process behaviour in wide deep neural networks. In *6th International Conference on Learning Representations, ICLR 2018-Conference Track Proceedings*.

[Domingos, 2020] Domingos, P. (2020). Every model learned by gradient descent is approximately a kernel machine. *arXiv preprint arXiv:2012.00152*.

[Fasshauer, 2011] Fasshauer, G. E. (2011). Positive definite kernels: past, present and future. *Dolomites Research Notes on Approximation*, 4:21–63.

[Fujimoto et al., 2018] Fujimoto, Y., Maruta, I., and Sugie, T. (2018). Input design for kernel-based system identification from the viewpoint of frequency response. *IEEE Transactions on Automatic Control*, 63(9):3075–3082.

[Iske, 2018] Iske, A. (2018). *Approximation Theory and Algorithms for Data Analysis*. Springer.

[Kanagawa et al., 2018] Kanagawa, M., Hennig, P., Sejdinovic, D., and Sriperumbudur, B. K. (2018). Gaussian processes and kernel methods: A review on connections and equivalences. *arXiv preprint arXiv:1807.02582*.

[Karimshoushtari and Novara, 2020] Karimshoushtari, M. and Novara, C. (2020). Design of experiments for nonlinear system identification: A set membership approach. *Automatica*, 119:109036.

[Knuth et al., 2021] Knuth, C., Chou, G., Ozay, N., and Berenson, D. (2021). Planning with learned dynamics: Probabilistic guarantees on safety and reachability via Lipschitz constants. *IEEE Robotics and Automation Letters*.

[Laurain et al., 2020] Laurain, V., Tóth, R., Piga, D., and Darwish, M. A. H. (2020). Sparse rkhs estimation via globally convex optimization and its application in LPV-IO identification. *Automatica*, 115:108914.

[Lauricella and Fagiano, 2020] Lauricella, M. and Fagiano, L. (2020). Set membership identification of linear systems with guaranteed simulation accuracy. *IEEE Transactions on Automatic Control*, 65(12):5189–5204.

[Lederer et al., 2020] Lederer, A., Capone, A., and Hirche, S. (2020). Parameter optimization for learning-based control of control-affine systems. In *Learning for Dynamics and Control*, pages 465–475. PMLR.

[Lederer et al., 2019] Lederer, A., Umlauft, J., and Hirche, S. (2019). Uniform error bounds for gaussian process regression with application to safe control. In *Conference on Neural Information Processing Systems (NeurIPS)*.

[Maddalena et al., 2020a] Maddalena, E. T., Scharnhorst, P., Jiang, Y., and Jones, C. N. (2020a). KPC: Learning-based model predictive control with deterministic guarantees. *arXiv preprint arXiv:2011.11303*.

[Maddalena et al., 2020b] Maddalena, E. T., Scharnhorst, P., and Jones, C. N. (2020b). Deterministic error bounds for kernel-based learning techniques under bounded noise. *Automatica (Provisionally accepted)*.

[Manton et al., 2015] Manton, J. H., Amblard, P.-O., et al. (2015). A primer on reproducing kernel Hilbert spaces. *Foundations and Trends in Signal Processing*, 8(1–2):1–126.

[Manzano et al., 2020] Manzano, J. M., Limon, D., de la Peña, D. M., and Calliess, J.-P. (2020). Robust learning-based MPC for nonlinear constrained systems. *Automatica*, 117:108948.

[Mei et al., 2019] Mei, S., Misiakiewicz, T., and Montanari, A. (2019). Mean-field theory of two-layers neural networks: dimension-free bounds and kernel limit. In *Conference on Learning Theory*, pages 2388–2464. PMLR.

[Micchelli et al., 2006] Micchelli, C. A., Xu, Y., and Zhang, H. (2006). Universal kernels. *Journal of Machine Learning Research*, 7(12).

[Milanese and Novara, 2004] Milanese, M. and Novara, C. (2004). Set membership identification of nonlinear systems. *Automatica*, 40(6):957–975.

[O’Hagan, 2004] O’Hagan, T. (2004). Dicing with the unknown. *Significance*, 1(3):132–133.

[Parzen et al., 1961] Parzen, E. et al. (1961). An approach to time series analysis. *Annals of mathematical statistics*, 32(4):951–989.

[Pillonetto et al., 2014] Pillonetto, G., Dinuzzo, F., Chen, T., De Nicolao, G., and Ljung, L. (2014). Kernel methods in system identification, machine learning and function estimation: A survey. *Automatica*, 50(3):657–682.

[Pin et al., 2015] Pin, G., Assalone, A., Lovera, M., and Parisini, T. (2015). Non-asymptotic kernel-based parametric estimation of continuous-time linear systems. *IEEE Transactions on Automatic Control*, 61(2):360–373.

[Raissi et al., 2004] Raissi, T., Ramdani, N., and Candau, Y. (2004). Set membership state and parameter estimation for systems described by nonlinear differential equations. *Automatica*, 40(10):1771–1777.

[Rasmussen and Williams, 2006] Rasmussen, C. E. and Williams, C. K. I. (2006). *Gaussian Processes for Machine Learning*. The MIT Press.

[Risuleo et al., 2017] Risuleo, R. S., Bottegal, G., and Hjalmarsson, H. (2017). A non-parametric kernel-based approach to Hammerstein system identification. *Automatica*, 85:234–247.

[Risuleo et al., 2019] Risuleo, R. S., Lindsten, F., and Hjalmarsson, H. (2019). Bayesian nonparametric identification of Wiener systems. *Automatica*, 108:108480.

[Rizvi et al., 2018] Rizvi, S. Z., Velni, J. M., Abbasi, F., Tóth, R., and Meskin, N. (2018). State-space LPV model identification using kernelized machine learning. *Automatica*, 88:38–47.

[Rosolia and Borrelli, 2017] Rosolia, U. and Borrelli, F. (2017). Learning model predictive control for iterative tasks. a data-driven control framework. *IEEE Transactions on Automatic Control*, 63(7):1883–1896.

[Schaback, 1995] Schaback, R. (1995). Error estimates and condition numbers for radial basis function interpolation. *Advances in Computational Mathematics*, 3(3):251–264.

[Schaback and Wendland, 2006] Schaback, R. and Wendland, H. (2006). Kernel techniques: from machine learning to meshless methods. *Acta numerica*, 15:543.

[Schölkopf, 2019] Schölkopf, B. (2019). Causality for machine learning. *arXiv preprint arXiv:1911.10500*.

[Schölkopf et al., 2002] Schölkopf, B., Smola, A. J., Bach, F., et al. (2002). *Learning with kernels: support vector machines, regularization, optimization, and beyond*. MIT press.

[Srinivas et al., 2012] Srinivas, N., Krause, A., Kakade, S. M., and Seeger, M. W. (2012). Information-theoretic regret bounds for Gaussian process optimization in the bandit setting. *IEEE Transactions on Information Theory*, 58(5):3250–3265.

[Umlauft and Hirche, 2019] Umlauft, J. and Hirche, S. (2019). Feedback linearization based on gaussian processes with event-triggered online learning. *IEEE Transactions on Automatic Control*, 65(10):4154–4169.

[Wabersich et al., 2021] Wabersich, K. P., Hewing, L., Carron, A., and Zeilinger, M. N. (2021). Probabilistic model predictive safety certification for learning-based control. *IEEE Transactions on Automatic Control*.

[Wendland, 2004] Wendland, H. (2004). *Scattered data approximation*, volume 17. Cambridge university press.

[Zhang et al., 2013] Zhang, Y., Duchi, J., and Wainwright, M. (2013). Divide and conquer kernel ridge regression. In *Conference on Learning Theory (COLT)*, pages 592–617. PMLR.